Gravitational lensing for stationary axisymmetric black holes in Eddington-inspired Born-Infeld gravity

Md Sabir Ali[*] and Shagun Kauhsal[†]

Indian Institute of Technology Ropar, Punjab-140001, India

(Received 13 September 2021; accepted 4 January 2022; published 24 January 2022)

Recent years have witnessed a surge of interest of the lensing of the black holes arising from general as well as other modified theories of gravity due to the experimental data available from the Event Horizon Telescope (EHT) results. The EHT may open a new door indicating the possible existence of the rotating black hole solutions in modified theories of gravity in the strong field regime. With this motivation, we investigate in the present paper the equatorial lensing ($\theta = \pi/2$) by a recently obtained exact rotating black holes solution in Eddington-inspired Born-Infeld (EiBI) theory in both the strong- and weak-field limits. Such black holes are the modification of Kerr-Newman black holes in general relativity, characterized by their mass M, the charge Q, and the rotation parameter a. and an additional term ϵ accounting for the correction to the Kerr-Newman solutions. We show numerically the variations of the impact parameter u_m, the light deflection coefficients p and q, and the total azimuthal bending angle α_D and find a close dependence of these quantities on the charge parameter r_q, the correction term ϵ, and the spin a. We also calculate the angular position θ_∞, the angular separation s, and the magnification of the relativistic images. In addition, we also discuss the weak lensing of the black holes in Eddington-inspired Born-Infeld (EiBI) theory using the Gauss-Bonnet theorem. We calculate the weak lensing parameter and find its variation with different values of the parameters r_q and ϵ.

DOI: 10.1103/PhysRevD.105.024062

I. INTRODUCTION

Einstein's general relativity admits only a few exact physically acceptable solutions [1]. Among these limited solutions, we have the axially symmetric stationary solutions, such as Kerr and Kerr-Newman, which are, respectively, the vacuum and electrovacuum solutions of general relativity [2–6]. These solutions are well established in the context of no-hair theorems for the asymptotically flat axisymmetric spacetimes. However, in the presence of hair, no-hair theorems may find other solutions which are characterized by some other parameters. An extension of this possibility has been done in the case of scalar and Proca hairs in the asymptotically de Sitter spacetimes [7]. It is also shown in another investigation that the no-hair theorem ruled out the possible existence of the real massive vector field in $f(R)$ theories as long as the potential due to the scalar field is positive definite in Einstein's frame [8]. To check the Kerr black holes hypothesis to know the exact nature of the astrophysical black holes is a proven fact that has been tested many times using x-ray spectroscopy of the accreting matter around the black holes [9,10], the strong gravitational lensing, and the recently obtained images of black holes silhouettes of M87 supermassive black holes using the Event Horizon Telescope (EHT) [11–16]. Apart from these, gravitational wave astronomy confirms that the gravitational waves emerging from black hole mergers using the Kerr solution strongly match with the waveform signals as detected by the LIGO Scientific and Virgo collaborations [17,18]. But these results may not find their validity in the strong gravity regime, and the alternative theories of gravity may find a new resource to test the strong gravity field with the more advanced future technologies [19]. The awakening of the gravitational wave astronomy by LIGO/Virgo and the imaging of the shadow of M87 black holes by the EHT may open a new door to the physics world, particularly in the strong gravity regime such as black hole physics. Since the astrophysical black holes are mostly rotating, thereby obtaining the exact rotating solutions in different gravity theories is a pressing topic to test the strong gravity regime through gravitational waves and imaging of black holes mostly residing presumably at the heart of every galaxy.

Having obtained a black hole solution, it is worth investigating one of the most prominent astrophysical events that occurred when light rays pass through such compact objects. The light rays or any massive particles while encountering the black holes, their direction of propagation drastically changes. Light rays, instead of following the straight path, would follow the curved path that black holes have created in their surroundings. Such a

[*]sabir.ali@iitrpr.ac.in
[†]2018phz0006@iitrpr.ac.in

phenomenon is called the gravitational lensing. After its first-ever imaging of the silhouettes of the M87 supermassive black holes by the EHT, the study of the lensing phenomena in the strong gravity region has been of utmost importance. The shadow imaging in the sky relies on the gravitational lensing of strong field as encompassed by light rays, thereby bearing the fingerprints of the geometry of the strong field gravity. After its first inception by Darwin [20], the studies on the lens equation and lensing phenomena of the astrophysical compact objects were triggered. Later Frittelli *et al.* [21] and then Virbhadra [22] analyzed the lens equation without referring to the black holes background. After that, the lens equation by Virbhadra and Ellis for the Schwarzschild black holes was constructed. In the subsequent years, Bozza *et al.* [23,24], following the Virbhadra-Ellis lens equation, invented a mathematical formulation of the gravitational lensing of a generic black hole in a spherically symmetric spacetime. Motivated by the formulation and with the advance of time, people made tremendous developments in the investigation of the strong gravitational lensing of the various static spherically symmetric as well as axially symmetric stationary black hole spacetimes [25–40]. The light bending phenomenon is analyzed to investigate and eventually to rule out possible inhomogeneity of the dark energy in the form of an ideal static fluid, within the maximum turnaround radius of a cosmic structure [41]. The bending angle and the perihelion precision of light for two different spherically symmetric spacetimes in Hordeski gravity theories in the realm of astrophysical scenarios also have been investigated [42]. The gravitational lensing by black holes has been investigated using both analytical and numerical techniques [22,34,40,43–59]. With the advent of modern technologies, the EHT group has been able to image the black holes silhouettes using very long baseline interferometry (VLBI) techniques [11–16]. They observed the very first image of the shadow of the M87 supermassive black holes by modeling the Kerr spacetime. These investigations from the EHT placed a strong piece of evidence at first sight that there could be no other spacetimes apart from the Kerr metric [11]. However, recently measured values of the rotation parameter show uncertainties to what could have been expected using the Kerr metric as a source [60]. Therefore, some minimal constraint conditions on the angular measurement of the Kerr black holes should be imposed [61]. Therefore, the non-Kerr black holes showing the significant deviations in measurement procedures cannot be a possible candidate from the phenomenological point of view [61].

There has been a lot of research interest in the investigations of the strong gravitational lensing for a non-Kerr family of black holes. The physical observables for the lensing effect in the strong domain of gravity have been investigated for various rotating non-Kerr spacetimes, e.g., the hairy Kerr black holes [62], the nonsingular Kerr-Sen black holes [59], the rotating black holes in $4D$ Einstein Gauss-Bonnet (EGB) gravity [63], etc. They studied rigorously various observables, such as the light deflection angle, the angular distance, and the angular separation and angular magnifications and also the time delay effects to investigate the astrophysical consequences in the context of the black holes M87 and SgrA* [64]. Motivated by these ideas, in this paper, we aim to discuss these physical observables for strong lensing for the rotating solution in the context of EiBI gravity theory. It is possible to test the strong field gravitational effects using such a non-Kerr family of black holes for a variety of observations.

The paper is organized as follows. In Sec. II, we briefly review the rotating black holes in Eddington-inspired Born-Infeld gravity. We give the usual formalism to derive the strong lensing observable in Sec. III. The numerical techniques and plots of the light deflection angle, the angular distance, and the angular separations are obtained in Sec. IV. The derivations of the weak-field light bending angle using the Gauss-Bonnet theorem is the subject of Sec. V. We conclude the paper in Sec. VI.

II. EIBI GRAVITY AND ROTATING SOLUTIONS

The rotating solutions in the Eddington-inspired Born-Infeld gravity are obtained when one employs the correspondence between modified models as a contraction of a metric tensor with the Ricci scalars formulated in light of general relativity and the Ricci-based gravity theories. For the basic investigations and the properties of the rotating black holes in EiBI gravity theories, we refer our reader to Ref. [64] and the references therein. This is an exact solution that is obtained when there is a nonminimal coupling to nonlinear electrodynamics of Born-Infeld gravity. The rotating black hole in Einstein-inspired Born-Infeld gravity theories in the usual Boyer-Lindquist coordinates (t, x, θ, ϕ) reads as [64]

$$ds^2 = -\left(1 - f + \epsilon\rho^q \frac{(\Delta + a^2\sin^2\theta)}{\Sigma}\right)dt^2 - 2a\left(f - \epsilon\rho^q \frac{(\Delta + x^2 + a^2)}{\Sigma}\right)\sin^2\theta dt d\phi + \frac{(1+\epsilon\rho^q)\Sigma}{\Delta}dx^2 + (1-\epsilon\rho^q)\Sigma d\theta^2 + \left[(x^2 + a^2 + fa^2\sin^2\theta) - \epsilon\rho^q \frac{(x^2+a^2)^2 + a^2\Delta\sin^2\theta}{\Sigma}\right]\sin^2\theta d\phi^2, \quad (1)$$

where the correction term ϵ encodes the deviation of charged rotating black holes in EiBI gravity to that of the Kerr-Newman metric of general relativity. We have also noted that

$$f = \frac{r_S x - r_q^2/2}{\Sigma} = \frac{x^2 + a^2 - \Delta}{\Sigma}$$
$$\Sigma = x^2 + a^2\cos^2\theta$$
$$\Delta = x^2 - r_S x + a^2 + r_q^2/2, \tag{2}$$

and

$$\rho^q = \frac{r_q^2}{2\Sigma^2}, \tag{3}$$

which can be viewed as the energy density of a charged rotating black holes whose electromagnetic field is described by

$$A_\mu = (A_t, 0, 0, A_\phi) = \frac{Qx}{\Sigma}(1, 0, 0, -a\sin^2\theta), \tag{4}$$

from which we can immediately get the required components of the field strength tensor $F_{\mu\nu} = \nabla_\mu A_\nu - \nabla_\nu A_\mu$. The quantity a is the spin angular momentum of the black holes, and r_q is the charge parameter. The rotating black holes (1) in EiBI gravity encompass the Kerr-Newman black hole when $\epsilon = 0$ and Kerr black holes in the case of $r_q = 0$. To calculate the various observables in the study of the strong lensing, we are in a position to introduce the dimensionless quantities

$$x \to \frac{x}{r_S}, \qquad a \to \frac{a}{r_S}, \qquad t \to \frac{t}{r_S}, \qquad r_q \to \frac{r_q}{r_S}; \tag{5}$$

with this, the metric (1) is recast as

$$ds^2 = -\left(1 - \tilde{f} + \epsilon\tilde{\rho}^q \frac{(\tilde{\Delta} + a^2\sin^2\theta)}{\tilde{\Sigma}}\right)dt^2 - 2a\left(\tilde{f} - \epsilon\tilde{\rho}^q \frac{(\tilde{\Delta} + x^2 + a^2)}{\tilde{\Sigma}}\right)\sin^2\theta dt d\phi + \frac{(1 + \epsilon\tilde{\rho}^q)\tilde{\Sigma}}{\tilde{\Delta}}dx^2$$
$$+ (1 - \epsilon\tilde{\rho}^q)\tilde{\Sigma}d\theta^2 + \left[(x^2 + a^2 + \tilde{f}x^2\sin^2\theta) - \epsilon\tilde{\rho}^q \frac{(x^2 + a^2)^2 + a^2\tilde{\Delta}\sin^2\theta}{\tilde{\Sigma}}\right]\sin^2\theta d\phi^2. \tag{6}$$

We have also noted that

$$\tilde{f} = \frac{x - r_q^2/2}{\tilde{\Sigma}} = \frac{x^2 + a^2 - \tilde{\Delta}}{\tilde{\Sigma}}$$
$$\tilde{\Sigma} = x^2 + a^2\cos^2\theta$$
$$\tilde{\Delta} = x^2 - x + a^2 + r_q^2/2 \tag{7}$$

and

$$\tilde{\rho}^q = \frac{r_q^2}{2\tilde{\Sigma}^2}, \tag{8}$$

The rotating black holes in EiBI gravity are stationary axially symmetric spacetimes which are invariant under the simultaneous transformation $t \to -t$ and $\phi \to -\phi + 2\pi$. Therefore, the metric (6) admits two Killing vectors, $\eta^\mu_{(t)} = \delta^\mu_t$ and $\eta^\mu_{(\phi)} = \delta^\mu_\phi$, which are linearly independent. The vectors $\eta^\mu_{(t)}$ and $\eta^\mu_{(\phi)}$ are associated, respectively, with the translational and rotational isometries [65]. The event horizon is a well-defined boundary that is a null hypersurface, and it comprises the outward null geodesics which are not capable of hitting the null infinity in the future. The event horizon is a solution of $g^{xx} = \tilde{\Delta} = 0$, which leads to the form

$$x_\pm = \frac{1 \pm \sqrt{1 - 4(a^2 + r_q^2/2)}}{2}. \tag{9}$$

which has the same expression as of the Kerr-Newman black holes. Therefore, the event horizon of the rotating black holes in EiBI black holes theory has structure similar to that of the Kerr-Newman black holes. However, the static limit surface is not the same as $g_{tt}^{\rm KN} \neq g_{tt}^{\rm EiBI}$. The black hole exists only in the limit when $a^2 \leq 1/4 - r_q^2/2$. The maximum value of the rotation parameter turns out to be $a = 0.5$, for $r_q = 0$. For any nonzero value of the parameter r_q, the rotation parameter has value less than 0.5. The left side of Fig. 1 shows the variation of the horizon $x_\pm$ with respect to the rotation parameter a. The blue dotted curve represents the Cauchy horizon, x_-, whereas the black solid line represents the event horizon, x_+. Similarly, the right figure shows the parameter space of the charge parameter r_q with respect to the rotation parameter a. The shaded region in this plot shows the no-black-hole spacetime. This figure shows the restricted theoretical values of r_q and a.

Given the opportunities available for testing the alternative theories of gravity, the physical implications of such black hole solutions and the analysis of their various features is very timely in the context of astrophysical settings. From the data available from various experimental setups such as the EHT, the LIGO Scientific Collaboration,

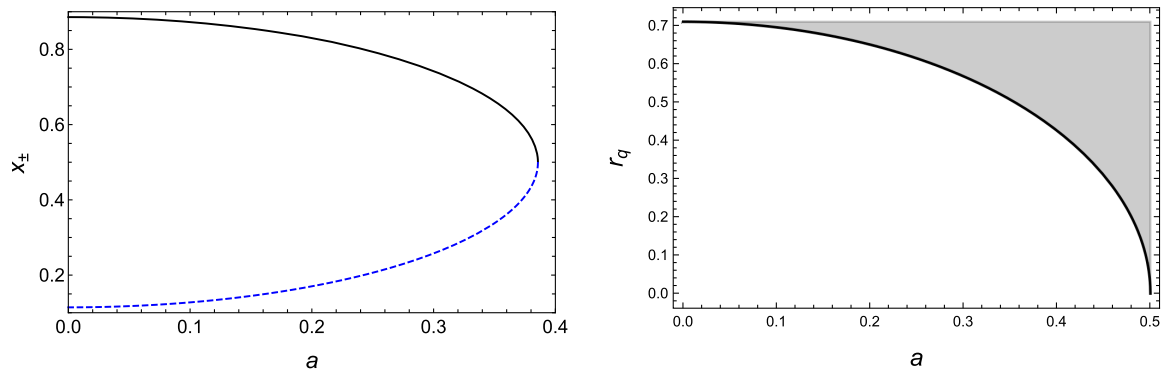

FIG. 1. The plot of horizon radius vs the rotation parameter for $r_q = 0.45$ (left) and the charge parameter vs the rotation parameter (right).

and the Virgo Collaboration, one can study the potential deviations of the Kerr-Newman black holes in general relativity in the study of accretion disks, strong gravitational lensing and shadows, generation of gravitational waves in binary mergers, and so on, from that of the rotating solutions that arise from the EiBI gravity.

III. EQUATORIAL BLACK HOLE LENSING

In this section, we investigate the equatorial ($\theta = \pi/2$) light bending due to the rotating black holes in EiBI gravity. The effects of the deformation parameter ϵ, the charge parameter r_q, and the spin a on the equatorial lensing will also be investigated. The metric (6) for the equatorial plane reads as

$$\mathrm{ds}^2 = -A(x)dt^2 + B(x)dx^2 + C(x)d\phi^2 - D(x)dtd\phi, \quad (10)$$

where

$$A(x) = \left(1 - \frac{1}{x} + \frac{r_q^2}{2x^2}\left(1 + \frac{\epsilon}{x^2}\left(1 - \frac{1}{x} + \frac{2a^2 + r_q^2/2}{2x^2}\right)\right)\right),$$
$$B(x) = \frac{x^2 + \frac{\epsilon r_q^2}{2x^2}}{\tilde{\Delta}},$$
$$C(x) = x^2 + a^2 + x - r_q^2/2 - \frac{\epsilon r_q^2}{2x^4}\frac{(x^2+a^2)^2 + a^2\tilde{\Delta}}{x^2},$$
$$D(x) = 2a\left(x - r_q^2/2 - \frac{\epsilon r_q^2}{2x^4}\frac{(x^2+a^2) + \tilde{\Delta}}{x^2}\right), \quad (11)$$

where $\tilde{\Delta} = x^2 + a^2 - x + r_q^2/2$. We write the Lagrangian

$$\mathcal{L} = g_{\mu\nu}\dot{x}^\mu\dot{x}^\nu, \quad (12)$$

which is used to find the geodesics equation. The overdot describes the derivative with respect to the affinely parametrized variable, say, λ. The metric (10) admits two Killing vectors due to time translation and rotation, which correspond, respectively, to the constant energy $\mathcal{E}$ and the constant angular momentum ℓ such that

$$2\mathcal{E} = \frac{\partial\mathcal{L}}{\partial\dot{t}} = g_{tt}\dot{t} + g_{t\phi}\dot{\phi}, \quad (13)$$

$$-2\ell = \frac{\partial\mathcal{L}}{\partial\dot{\phi}} = g_{t\phi}\dot{t} + g_{\phi\phi}\dot{\phi}. \quad (14)$$

We consider $\mathcal{E} = 1$ by suitably choosing the affine parameter and identify ℓ as the angular momentum of the photon with respect to the black hole axis. We have four first-order differential equations in the equatorial plane using Eqs. (13) and (14) and also the null geodesics conditions $ds^2 = 0$ as

$$\dot{t} = \frac{4C - 2\ell D}{4AC + D^2}, \quad (15)$$

$$\dot{\theta} = 0, \quad (16)$$

$$\dot{\phi} = \frac{2D + 4A\ell}{4AC + D^2}, \quad (17)$$

$$\dot{x} = \pm 2\sqrt{\frac{C - D\ell - A\ell^2}{B(4AC + D^2)}}. \quad (18)$$

Since we are interested in the study of the photon trajectories in the isolated black hole system, we can safely ignore the effect of the other celestial objects on the trajectory of the photon and can well approximate the spacetime as Minkowskian at a large enough distance. We assume that both the source and the observer are situated at a large distance from the black holes under study. This will satisfy our purpose for studying the lensing phenomena on the equatorial plane.

Now, we need to focus on the effective potential for light rays, V_{eff}, which they follow in the radial direction only. The effective potential follows from the relation $\dot{x}^2 + V_{\mathrm{eff}}(x) = 0$ and is given by

$$V_{\mathrm{eff}}(x) = -\frac{4(C - D\ell - A\ell^2)}{B(4AC + D^2)}. \quad (19)$$

At this point, it is worth it to understand that in the asymptotic limit the photons emanating from infinity approaches the black hole event horizon at some distance x_0 and leaves for infinity again. The impact parameter $u = \ell/\mathcal{E} = \ell$ ($\mathcal{E} = 1$) is defined in the equatorial plane. Therefore, for $V_{\text{eff}} = 0$, the expression for the angular momentum ℓ reads

$$\begin{aligned}\ell = u &= \frac{-D_0 + \sqrt{D_0^2 + 4A_0C_0}}{2A_0}, \\ &= \frac{\epsilon(4a^3 {r_q}^2 + a {r_q}^4 + 4a {r_q}^2 {x_0}^2 - 2a {r_q}^2 x_0) + \sqrt{2}{x_0}^2\sqrt{(2a^2 + {r_q}^2 + 2(x_0-1)x_0)(4{x_0}^8 - {r_q}^4\epsilon^2)}}{\epsilon(4a^2 {r_q}^2 + {r_q}^4 + 2{r_q}^2 {x_0}^2 - 2{r_q}^2 x_0) + 2{r_q}^2 {x_0}^4 + 4(x_0-1){x_0}^5} \\ &\quad + \frac{2a{r_q}^2 {x_0}^4 - 4a{x_0}^5}{\epsilon(4a^2 {r_q}^2 + {r_q}^4 + 2{r_q}^2 {x_0}^2 - 2{r_q}^2 x_0) + 2{r_q}^2 {x_0}^4 + 4(x_0-1){x_0}^5}.\end{aligned} \tag{20}$$

Hence, the expression for the impact parameter u can be obtained once we get the expression for x_0. The "+" sign in front of the square root is meant for $a > 0$, which indicates the prograde motion for light rays, and for $a < 0$, we have retrograde motion. The light deflection angle in a generic stationary axisymmetric spacetime for x_0 is expressed as

$$\alpha_D(x_0) = I(x_0) - \pi, \tag{21}$$

where the total azimuthal angle $I(x_0)$ reads

$$I(x_0) = 2\int_{x_0}^{\infty} \frac{d\phi}{dx} dx = 2\int_{x_0}^{\infty} P_1(x, x_0) P_2(x, x_0) dx, \tag{22}$$

$$\begin{aligned}P_1(x, x_0) &= \frac{\sqrt{B}(2A_0AL + A_0D)}{\sqrt{CA_0}\sqrt{4AC + D^2}}, \\ P_2(x, x_0) &= \frac{1}{\sqrt{A_0 - A\frac{C_0}{C} + \frac{L}{C}(AD_0 - A_0D)}}.\end{aligned} \tag{23}$$

The light rays follow a straight line along the geodesics when no black hole is present, thereby indicating $I(x_0) = \pi$. For a specific value of x_0, one can get $\alpha_D(x_0) = 2\pi$, which means that the light rays would complete a whole circular loop. It goes on decreasing, which eventually leads to forming more than one complete loop, and at a certain radius, say, $x_0 = x_m$, the total azimuthal deflection becomes infinitely large, and the light rays will be impinged into the black hole. This quantity x_m is called the unstable light rays' circular radius. An explicit expression for the integral (22) is not obtained. Therefore, following the method as developed by Bozza [24], we calculate the behavior of the deflection angle near the unstable photon orbit radius. In this respect, we define a new variable to separate the divergent and regular parts in $I(x_0)$, such that [24]

$$z = 1 - \frac{x_0}{x}. \tag{24}$$

With this definition the quantity $I(x_0)$ is now expressed as

$$I(x_0) = \int_0^1 R(z, x_0) f(z, x_0) dz, \tag{25}$$

where

$$R(z, x_0) = \frac{2x^2}{x_0} P_1(x, x_0), \tag{26}$$

$$f(z, x_0) = P_2(x, x_0). \tag{27}$$

The function $R(z, x_0)$ in $I(x_0)$ is nonsingular in nature for any value of z and x_0, whereas the function $f(z, x_0)$ is divergent at $z = 0$. To show explicitly the nature, we can Taylor expand the denominator of the function $f(z, x_0)$ in z such that

$$f(z, x_0) \sim f_0(z, x_0) = \frac{1}{\sqrt{\alpha z + \gamma z^2 + \mathcal{O}(z^3)}}, \tag{28}$$

where we have considered the expansion up to z^2 only. The parameters α and γ are given as

$$\alpha = \frac{x_0}{C_0}[(C_0'A_0 - A_0'C_0) + L(A_0'D_0 - A_0D_0')] \tag{29}$$

$$\begin{aligned}\gamma &= \frac{x_0}{2C_0^2}[2C_0(A_0C_0' - A_0'C_0) + 2x_0C_0'(C_0A_0' - A_0C_0') - x_0C_0(C_0A_0'' - A_0C_0'')] \\ &\quad + L\left[\frac{x_0^2C_0'(A_0D_0' - D_0A_0')}{{C_0}^2} + \frac{(x_0^2/2)(D_0A_0'' - A_0D_0'') + x_0(D_0A_0' - A_0D_0'))}{C_0}\right].\end{aligned} \tag{30}$$

Now, we find the photon orbit radius x_m, as the largest real root of the Eq. (29), such that

$$\begin{aligned}&-16a^4({r_q}^6\epsilon^3-12{r_q}^2x_0^8\epsilon)-4a^2(8x_0^{12}(x_0-{r_q}^2)-36{r_q}^2x_0^8\epsilon({r_q}^2+2(x_0-1)x_0)\\&+3{r_q}^6\epsilon^3({r_q}^2+2(x_0-1)x_0)-2{r_q}^4x_0^4\epsilon^2({r_q}^2+x_0(4x_0-3)))-(-{r_q}^6\epsilon^2+{r_q}^4x_0\epsilon(8x_0^3+\epsilon)\\&+4{r_q}^2x_0^5(x_0^3+4(x_0-1)\epsilon)-4x_0^9)(2\sqrt{2}a-8\sqrt{2}a^3{r_q}^2\epsilon(6x_0^4-{r_q}^2\epsilon))\sqrt{2\tilde{\Delta}_0(4x_0^8-{r_q}^4\epsilon^2)}\\&-({r_q}^2+2(x_0-1)x_0)({r_q}^2\epsilon+2x_0^4)(2{r_q}^6\epsilon^2+{r_q}^4x_0\epsilon(-8x_0^3+2x_0\epsilon-3\epsilon)\\&-8{r_q}^2x_0^5(x_0^3+2(x_0-1)\epsilon)+4(3-2x_0)x_0^9)=0,\end{aligned}\tag{31}$$

where $\tilde{\Delta}_0$ is the value of $\tilde{\Delta}$ at $x=x_0$. When one solves Eq. (31), one can get the value of the quantity x_m as a function of a, r_q, and ϵ. The dependence of the spin a on x_m has been depicted in Fig. 2 for a set of values of ϵ and r_q.

In the limit $x_0 \to x_m$, the quantity $\alpha = 0$, and consequently, we have $f(z,x_0) \approx 1/z$; thereby, the integral (25) becomes infinitely large as $z \to 0$. We write the integral (25) as a combination of divergence and regular parts such that

$$I(x_0) = I_D(x_0) + I_R(x_0),\tag{32}$$

with

$$I_D(x_0) = \int_0^1 R(0,x_m) f_0(z,x_0)\,dz,\tag{33}$$

$$I_R(x_0) = \int_0^1 [R(z,x_0)f(z,x_0) - R(0,x_0)f_0(z,x_0)]\,dz.\tag{34}$$

The integral (33) has an analytical solution:

$$I_D(x_0) = \frac{2R(0,x_m)}{\sqrt{\gamma}}\log\left(\frac{\sqrt{\gamma+\alpha}+\sqrt{\gamma}}{\sqrt{\alpha}}\right).\tag{35}$$

As $\alpha = 0$ at $x_0 = x_m$, the right-hand side of Eq. (33) has a infinity at $x_0 = x_m$, as can be seen from the expression inside the logarithm above. Therefore, the regular part is

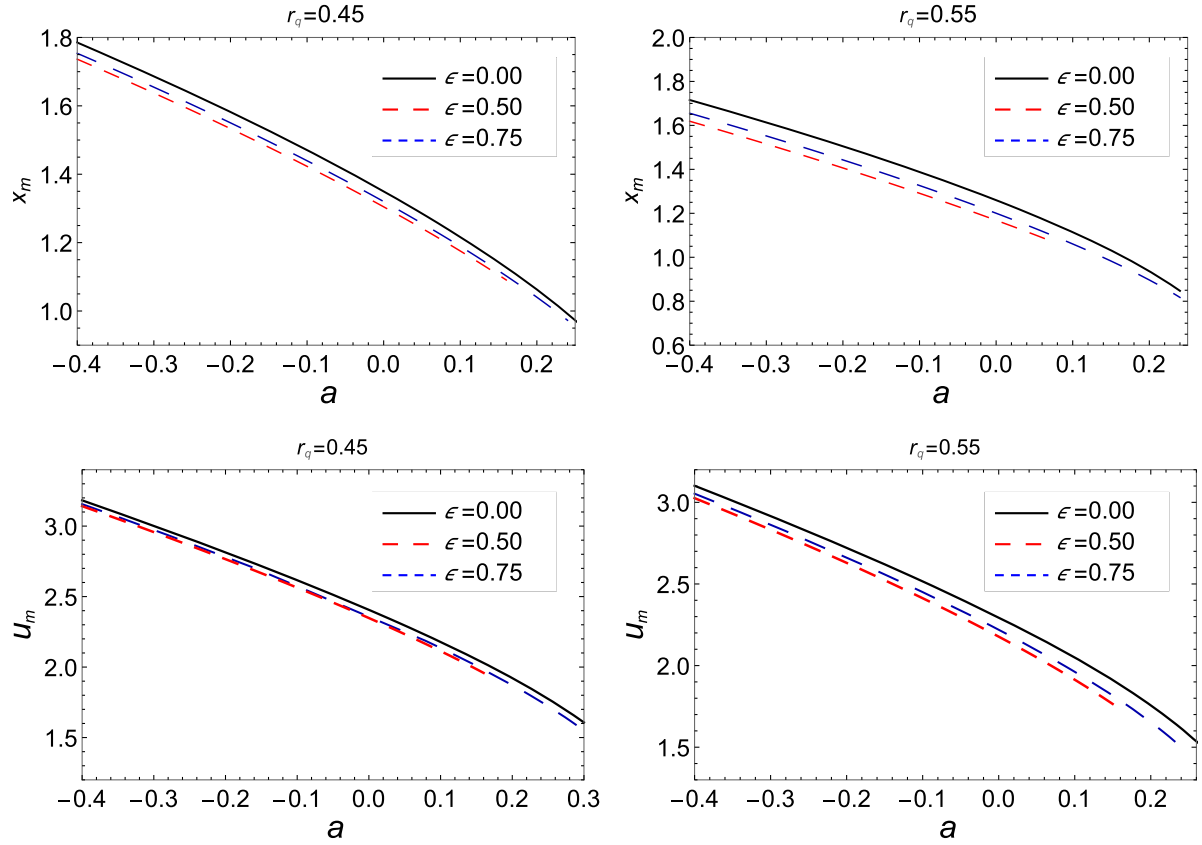

FIG. 2. Plot showing the variation of the photon orbit radius x_m (upper panel) and the impact parameter u_m (lower panel) with respect to the rotation parameter a for different values of r_q and ϵ.

contained in the integral of Eq. (34). Since it has significant contribution up to order of $(x_0 - x_m)$, we can take the regular parts as

$$I_R(x_m) = \int_0^1 [R(z, x_m) f(z, x_m) - R(0, x_m) f_0(z, x_m)] dz, \tag{36}$$

whose behavior can be seen from the numerical plots, Fig. 4. Now, using Eqs. (35) and (36), we express the quantity α_D as

$$\alpha_D(\theta) = -p \log\left(\frac{\theta D_{OL}}{u_m} - 1\right) + q + \mathcal{O}(u - u_m), \tag{37}$$

where the quantities p and q in Eq. (37) for the strong gravitational field limit are cast as

$$p = \frac{R(0, x_m)}{2\sqrt{\gamma_m}}, \quad \text{and} \quad q = -\pi + I_R(x_m) + p \log \frac{c x_m^2}{u_m^2}, \tag{38}$$

which is a polynomial of various parameters and is expressed as

$$p = \frac{2\sqrt{(r_q{}^2\epsilon + 2x_0{}^4)(2r_q{}^2(2a^2\epsilon + x_0{}^4 + (x_0 - 1)x_0\epsilon) + r_q{}^4\epsilon + 4(x_0 - 1)x_0{}^5)}}{\sqrt{2a^2 + r_q{}^2 + 2(x_0 - 1)x_0}\sqrt{c_1\gamma_m}}, \tag{39}$$

where

$$\begin{aligned} c_1 = {} & 2x_0{}^4(a^2(2x_0(x_0 + 1) - r_q{}^2) + 2x_0{}^4) \\ & - r_q{}^2\epsilon(4a^4 + a^2(r_q{}^2 + 2x_0(3x_0 - 1)) + 2x_0{}^4). \end{aligned} \tag{40}$$

Series expanding Eq. (20) in terms of $(x_0 - x_m)$, we have

$$u - u_m \approx c_2(x_0 - x_m)^2. \tag{41}$$

The analytical expression for c_2 is very large, and we do not write it here. We use the expression of c_2 in the numerical

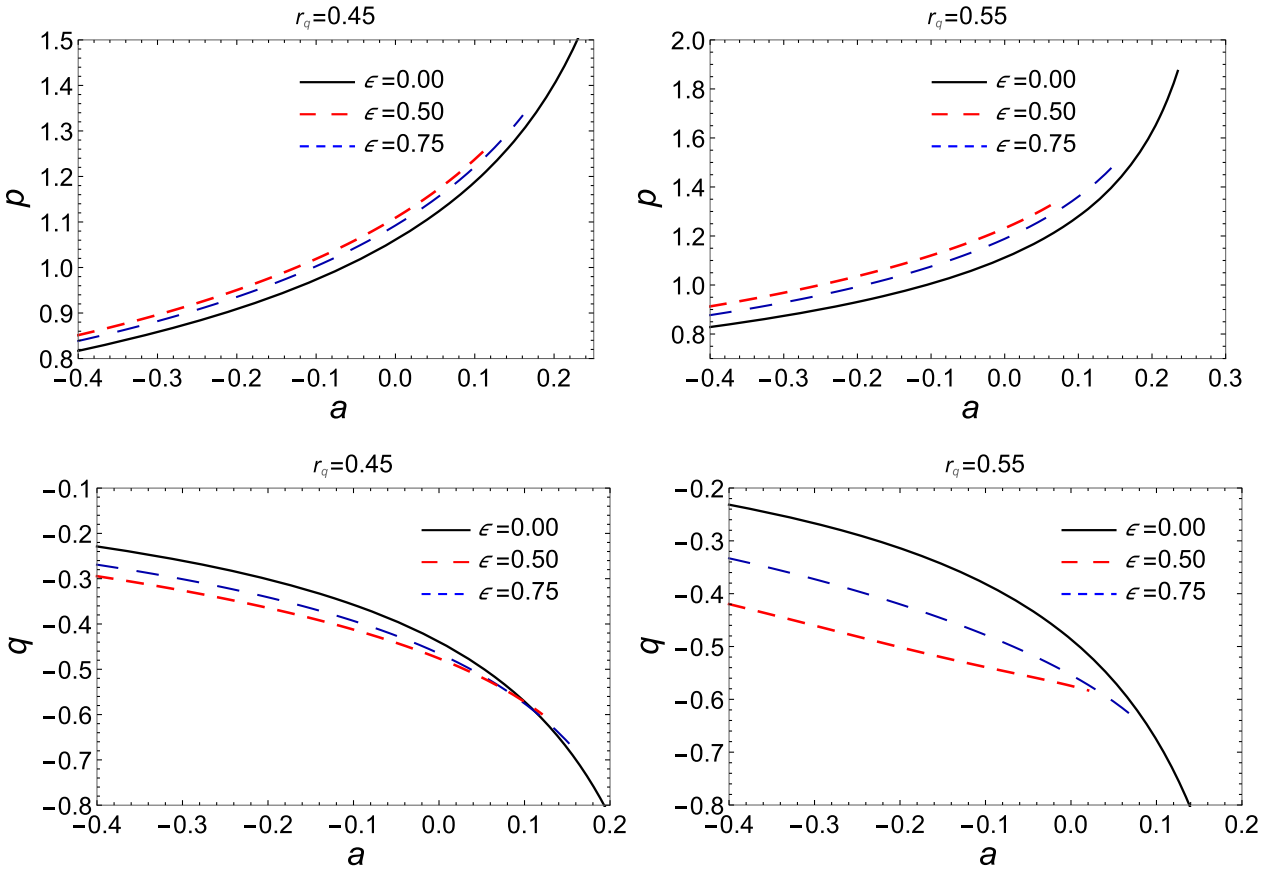

FIG. 3. The behavior of the deflection coefficient p vs the spin a (upper panel) and the variation of the coefficient q with spin a (lower panel) for different values of r_q and ϵ.

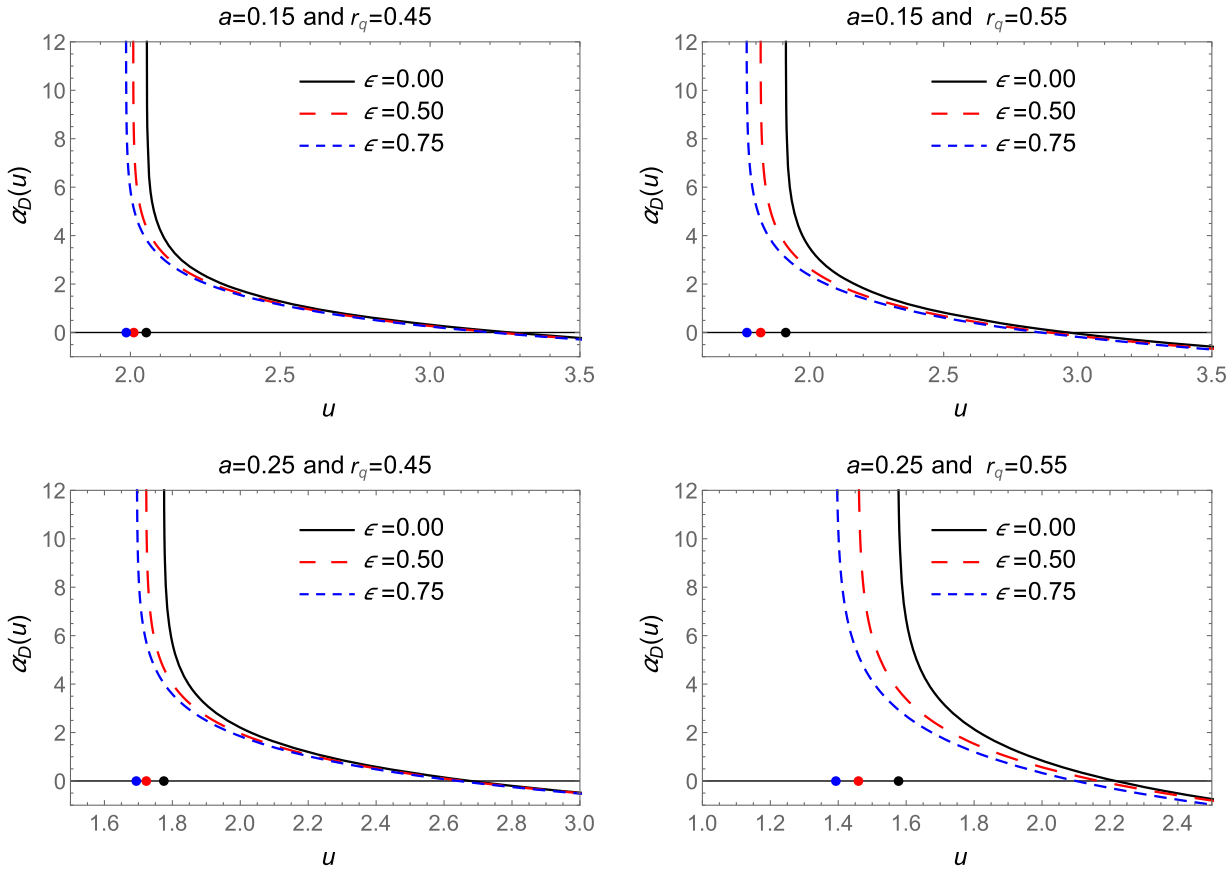

FIG. 4. Plot showing the behavior of the light deflection angle for different values of r_q and ϵ. Points on the horizontal shows the divergence of the deflection angle at $u = u_m$.

investigations of the light deflection coefficients p and q. Remember that all the expressions with the subscript m are obtained at $x_0 = x_m$. The quantities p and q, in Eq. (39), appear in the calculation of the total azimuthal angle, and they are called the deflection coefficients in the strong-field regime. We plot them in Fig. 3, which depicts that p and q show the opposite behavior with the different values of spin parameter a. As expected, these quantities become infinitely large as we increase the values of a, thereby indicating the validity of the coefficients at higher rotation parameter ceases to exist. As a limiting case, those results of strong-field deflection coefficients reduce to the corresponding limits of Kerr-Newman black holes when $\epsilon \to 0$, the Kerr black holes when $r_q \to 0$, and also the Schwarzschild black holes when $a \to 0$, $r_q \to 0$, and $\epsilon \to 0$.

IV. OBSERVABLES AND RELATIVISTIC IMAGES

In this section, we discuss about the strong gravitational lensing with the help of lens equations. There exist several methods to describe the lens equations, as they principally dependent on different choices of the variables. In describing the gravitational lensing, we place the black hole at the origin such that at one side there is the observer and at another side there is the light source. The light rays coming from the illuminating source (S) deviate from their original path while passing the black hole (L) due to the curvature and ultimately reach the observer (O). The line connecting the black holes and the observer and the image that the observer sees is an optical axis OL, and it will be deviated at an angle θ with respect to OL. Similarly, the light source will be aligned at β angle with OL. The emitted light rays make an angle $\alpha_D(\theta)$ when detected by the observer.

As mentioned earlier, there are various mathematical formulations to interpret the lensing phenomena. Among them, the Ohanian lens equation is the best approximation [54] to describe the positions of observer and the source as

$$\xi = \frac{D_{OL} + D_{LS}}{D_{LS}}\theta - \alpha_D(\theta), \tag{42}$$

where the angle $\xi \in [-\pi, \pi]$ connects the optical axis and the source directions. D_{OL} is the lens to the observer distance, while D_{LS} is the lens to source distance. The angles ξ and β are found to follow the relation [54,63]

$$\frac{D_{OL}}{\sin(\xi - \beta)} = \frac{D_{LS}}{\sin\beta}. \tag{43}$$

For the completeness of the above relations, we choose θ, ξ, and β to be tinier because in this case the relativistic images formed by the black holes are prominent. The light rays come from source S and make many loops while encountering the black holes, so the deflection angle α is replaced by $2n\pi + \Delta\alpha_n$, where the integer $n \in N$ represents the number that counts the loops and $0 < \Delta\alpha_n \ll 1$. Equation (42), together with Eq. (43) for smaller values of θ, is rewritten as

$$\beta = \theta - \frac{D_{LS}}{D_{OL} + D_{LS}}\Delta\alpha_n. \tag{44}$$

Next, Eq. (44) is utilized to extract the information regarding the image positions. For a critical impact parameter u_m, which is a function of the distance of the photon orbit radius x_m, $\alpha_D(\theta)$ becomes infinitely large. For each loop of the light rays, there is a certain value of the impact parameter, u, at which the light rays reaches from source to the observer. Therefore, on both sides of the black holes, an infinite number of relativistic images are constructed. Now, Eq. (37) with $\alpha_D({\theta_n}^0) = 2n\pi$ reads as

$${\theta_n}^0 = \frac{u_m}{D_{OL}}(1 + e_n), \tag{45}$$

where

$$e_n = e^{\frac{q-2n\pi}{p}}. \tag{46}$$

The Taylor expansion of the deflection angle $\alpha_D(\theta)$ around ${\theta_n}^0$ to the first order in $(\theta - {\theta_n}^0)$ reads [63]

$$\alpha_D(\theta) = \alpha_D({\theta_n}^0) + \left.\frac{\partial\alpha_D(\theta)}{\partial\theta}\right|_{{\theta_n}^0}(\theta - {\theta_n}^0) + \mathcal{O}(\theta - {\theta_n}^0). \tag{47}$$

On utilizing Eq. (45) and defining $\Delta\theta_n = (\theta - {\theta_n}^0)$, one gets

$$\Delta\alpha_n = -\frac{pD_{OL}}{u_m e_n}\Delta\theta_n. \tag{48}$$

Now, the final expression for the lens equation (44) reads [63]

$$\beta = ({\theta_n}^0 + \Delta\theta_n) + \frac{D_{LS}}{D_{OL} + D_{LS}}\left(\frac{pD_{OL}}{u_m e_n}\Delta\theta_n\right). \tag{49}$$

Substituting the value of $\Delta\theta_n = (\theta - {\theta_n}^0)$ and then ignoring the second term in Eq. (49) as it contributes much less than compared to the second term, we have

$$\theta_n = {\theta_n}^0 + \frac{D_{OL} + D_{LS}}{D_{LS}}\frac{u_m e_n}{D_{OL}p}(\beta - {\theta_n}^0). \tag{50}$$

Next, we discuss the most striking features of the gravitational lensing, the formation of the Einstein's ring. Einsten's rings are formed when we have the point lens perfectly aligned in the line of sight of the source such that the light from the source is spreading in all directions equally. The complex lens systems may lead to the formation of multiple Einstein rings [22,54,56]. Moreover, a partial double Einstein ring was also found in Ref. [57] in which the authors mentioned that these rings are created from two sources located at different distances from the lens. The relativistic Einstein's rings are formed when the deflection angle $\alpha \geq 2\pi$. For the lens and the observer to be perfectly oriented ($\beta = 0$) and the lens to be situated perfectly at the center of the observer and the source, then Eq. (50) reads [63]

$$\theta_n^E = \left(1 - \frac{2u_m e_n}{D_{OL}p}\right)\left(\frac{u_m}{D_{OL}}(1 + e_n)\right). \tag{51}$$

For $D_{OL} \gg u_m$, the angular radius () for Einstein's ring reduces to

$$\theta_n^E = \frac{u_m}{D_{OL}}(1 + e_n). \tag{52}$$

It is worth it to mention that θ_1^E is the angular position of the outermost ring. Figure 5 depicts the angular position θ_1^E various black holes. Like Einstein's, one of the most important quantities is the image magnification, which is viewed as the ratio of solid angles made by the image and the source with the central object, such that for the nth image the magnification is defined as [24,58]

$$\mu_n = \frac{1}{\beta}\left[\frac{u_m}{D_{OL}}(1 + e_n)\left(\frac{D_{OS}}{D_{LS}}\frac{u_m e_n}{D_{OL}p}\right)\right]. \tag{53}$$

As expected, the magnification decreases, and the image becomes fainter as n increases. We have from Ref. [24] the

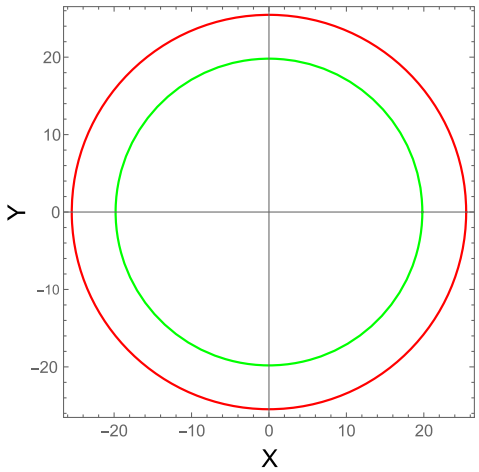

FIG. 5. Plots for the outermost Einstein rings for black holes at the center of nearby galaxies in the framework of Schwarzschild geometry. The red line corresponds to SgrA*, and green line corresponds to $M87$ [63].

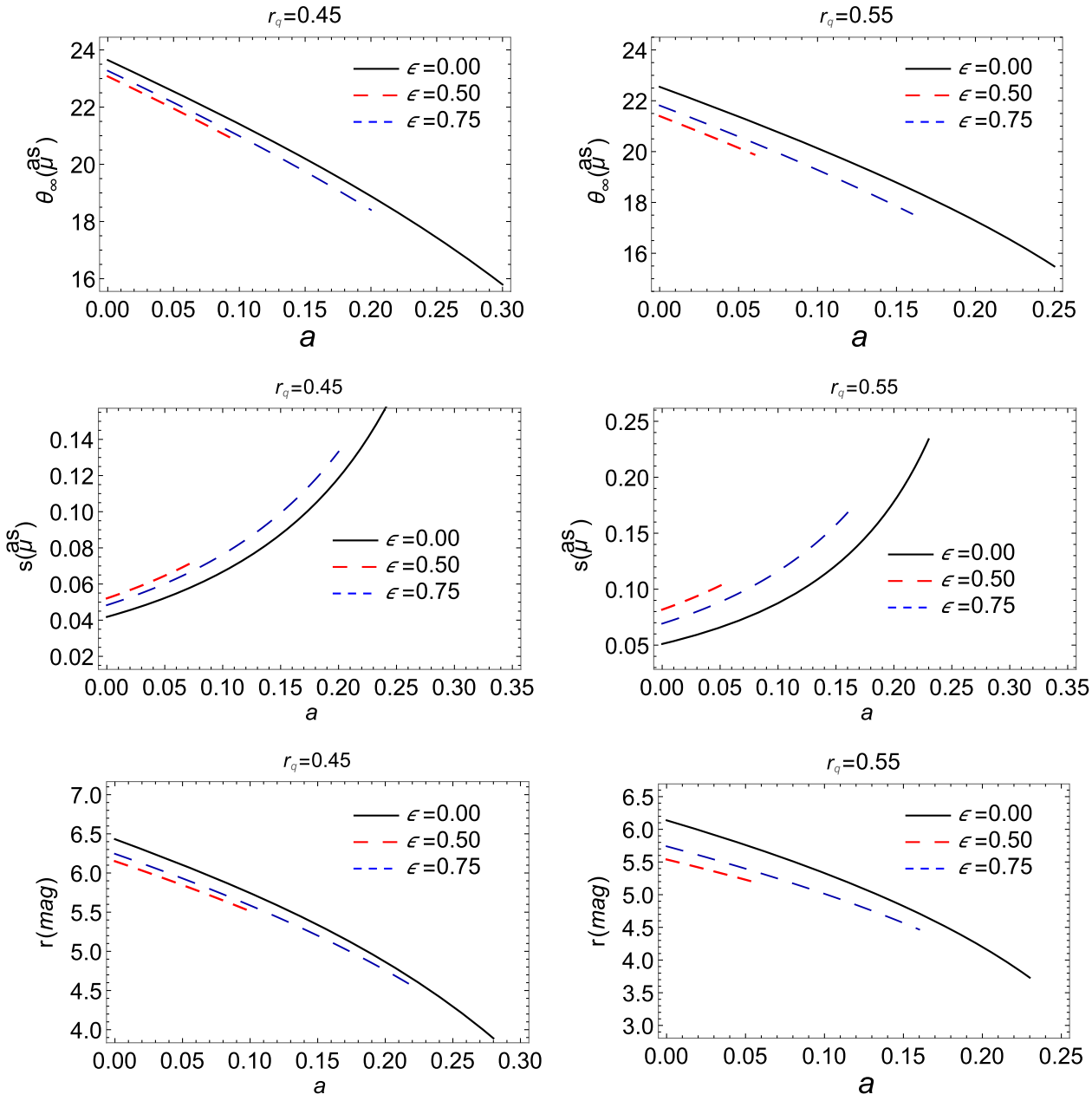

FIG. 6. Plot showing the variation of lensing observables θ_∞, s, and $r_{\rm mag}$ as a function of a for different values of r_q and ϵ for SgrA*.

important observables describing the rotating black holes in EiBI gravity theory as

$$\theta_\infty = \frac{u_m}{D_{OL}} \tag{54}$$

$$s = \theta_1 - \theta_\infty \approx \theta_\infty (e^{\frac{q-2p}{p}}) \tag{55}$$

$$r_{\rm mag} = \frac{\mu_1}{\sum_{n=2}^{\infty} \mu_n} \approx e^{\frac{2p}{p}}, \tag{56}$$

where s is the angular separation between the first image ($n = 1$) and the rest of the images which are supposedly packed at θ_∞, $r_{\rm mag}$ is the ratio of the flux magnification of the first image and sum of the flux magnification of all the other images. We plot these observables in a realistic scenario of various black holes, such as the Sgr A*, M87 [66]. We consider $M = 4.3 \times 10^6\ M_\odot$ and $d = 8.35$ Kpc [67] for Sgr A* and $M = 6.5 \times 10^9\ M_\odot$ and $d = 16.8$ Mpc for M87 [16]. From the plots in Figs. 6 and 7 it is clear that the angular separation increases but the angular position (θ_∞) and the flux magnitude ($r_{\rm mag}$) decrease with different values of r_q and ε.

We tabulated the values of the pair $(a, 2\theta_\infty)$ for a fixed value of the rotation parameter $r_q/r_S = 0.15$ (one should remember that $r_S = 2M$ is the Schwarzschild radius, where M is the mass of the EiBI black hole). We can estimate the value of the deflection angle for M87 black holes using the

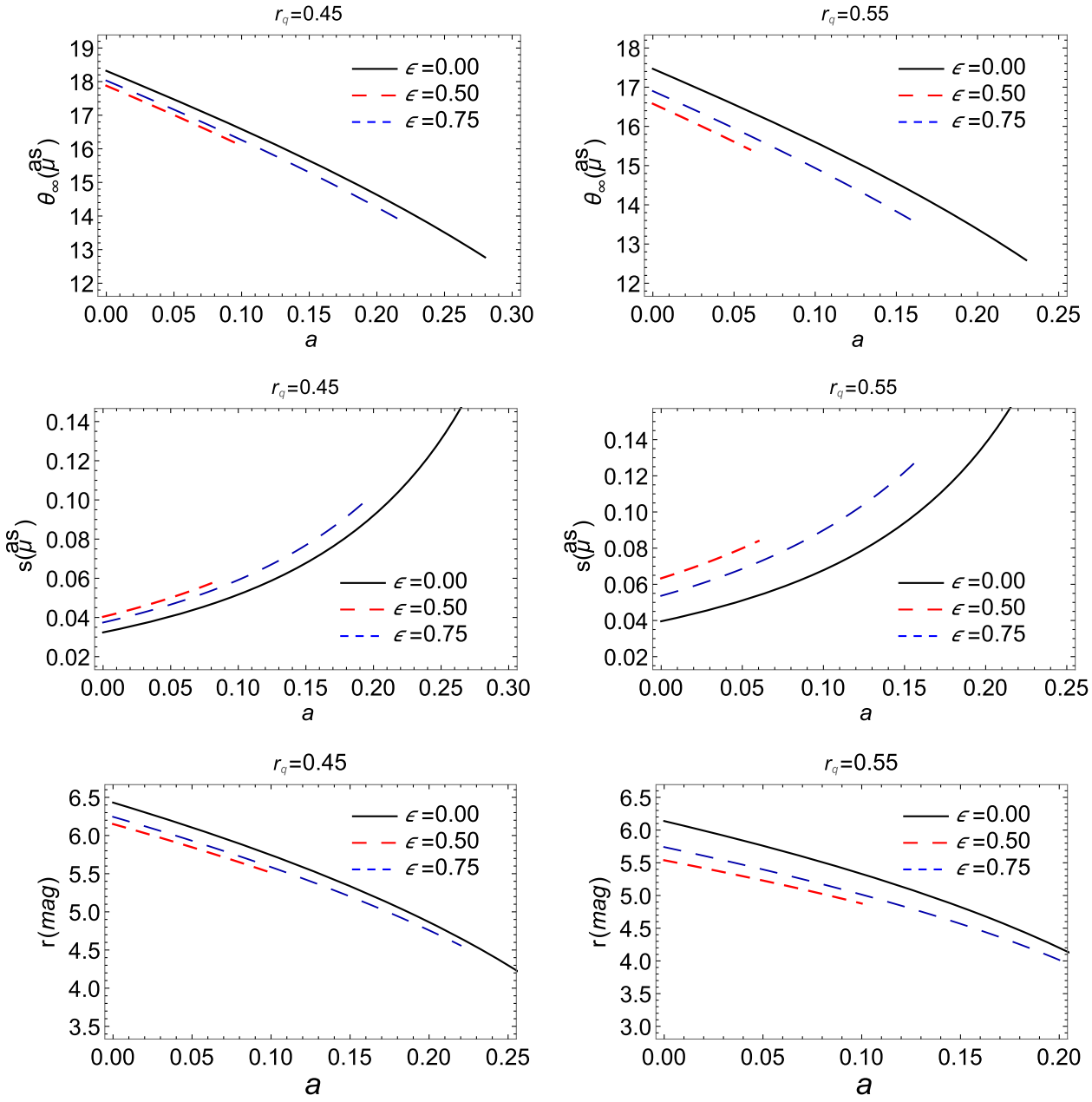

FIG. 7. Plot showing the variation of lensing observables θ_∞, s, and $r_{\rm mag}$ as a function of a for different values of r_q and ϵ for M87.

restricted values of the parameters r_q and ϵ. If we assume the parametric values of these parameters as tabulated in Table I, we can see that we have the diameter of the photon ring of the M87 black holes as reported by the EHT Collaboration. Although, we do not get the upper bound of the diameter of the photon ring, i.e., 45 μas, as reported by EHT, we get the values 42 and 39 μas, as the bound lies as 42 ± 3 μas (see the tabulated values for the M87 black holes for the reference).

For a consistency check, we have also calculated the diameter of the photon ring of the SgrA*. We see that if we allow the window of $2\theta_\infty = 42 \pm 3$ μas for the diameter of the photon ring for the SgrA* then, for the particular values of the parameters r_q and a, we always have the satisfactory results. We have tabulated them in Table II.

V. WEAK GRAVITATIONAL LENSING

In the present section, we deal with the weak lensing of the rotating charged black holes in EiBI theory. We rewrite the metric in usual (t, r, θ, ϕ) coordinates to get the form

$$ds^2 = -X(r,\theta)dt^2 - 2U(r,\theta)dtd\phi + Y(r,\theta)dr^2 + Z(r,\theta)d\theta^2 + V(r,\theta)d\phi^2, \quad (57)$$

where the form of $X(r,\theta)$, $Y(r,\theta)$, $Z(r,\theta)$, $V(r,\theta)$, and $U(r,\theta)$ can be seen when we compare the metric (1)

TABLE I. The table shows the set values of the spin parameter a and the full deflection angle, i.e., $a, 2\theta_\infty$ of rotating EiBI black hole with the charge parameter $r_q/r_S = 0.15$, and $\epsilon/r_S^2 = 0.0$ (first column), $\epsilon/r_S^2 = 0.1$ (second column), and $\epsilon/r_S^2 = 0.15$ (third column) as a model to the M87 black holes.

$a, 2\theta_\infty(\mu\text{as})$	$a, 2\theta_\infty(\mu\text{as})$	$a, 2\theta_\infty(\mu\text{as})$
(0.0,42.285)	(0.0, 42.2752)	(0.0, 42.2703)
(0.0104,42)	(0.0102,42)	(0.0084, 42)
(0.05,40.6065)	(0.05, 40.5963)	(0.05, 40.5912)
(0.0963,39)	(0.0963, 39)	(0.0960, 39)
(0.1,38.8696)	(0.1, 38.859)	(0.1, 38.8536)
(0.15,37.06241)	(0.15, 37.0513)	(0.15, 37.0457)
(0.2,35.1682)	(0.2,35.1566)	(0.2, 35.1507)
(0.25,33.1626)	(0.25,33.1504)	(0.25, 33.1442)
(0.3,31.0074)	(0.3, 30.9945)	(0.3, 30.988)
(0.35,28.6361)	(0.35, 28.6225)	(0.35, 28.6157)
(0.4,25.9127)	(0.4,25.8985)	(0.4, 25.8914)
(0.45,22.4438)	(0.45, 22.4298)	(0.45, 22.4228)

TABLE II. The table shows the set values of the spin parameter a and the full deflection angle, i.e., $(a, 2\theta_\infty)$ of a rotating EiBI black hole with the charge parameter $r_q/r_S = 0.15$, and $\epsilon/r_S^2 = 0.0$ (first column), $\epsilon/r_S^2 = 0.1$ (second column), and $\epsilon/r_S^2 = 0.15$ (third column) as a model to the SgrA*.

$(a, 2\theta_\infty(\mu\text{as}))$	$(a, 2\theta_\infty(\mu\text{as}))$	$(a, 2\theta_\infty(\mu\text{as}))$
(0.0,50.6784)	(0.0, 50.6666)	(0.0, 50.6608)
(0.05,48.6666)	(0.05, 48.6544)	(0.05, 48.6483)
(0.1,46.585)	(0.1, 46.5722)	(0.1, 46.5659)
(0.1361,45)	(0.136, 45)	(0.1363, 45)
(0.15,44.4191)	(0.15, 44.4058)	(0.15, 44.3991)
(0.2,42.1489)	(0.2, 42.1349)	(0.2, 42.1279)
(0.2031,42)	(0.202, 42)	(0.204,42)
(0.25,39.7452)	(0.25,39.73057)	(0.25, 39.723)
(0.2648,39)	(0.26420, 39)	(0.265, 39)
(0.3,37.1622)	(0.3, 37.1467)	(0.3, 37.1389)
(0.35,34.3202)	(0.35,34.3039)	(0.35,34.2958)
(0.4,31.0562)	(0.4, 31.0392)	(0.4, 31.0306)
(0.45,26.8988)	(0.45, 26.882)	(0.45, 26.8736)

with (57). We consider only the null rays for the propagation, which is seen by computing $ds^2 = 0$ for dt as

$$dt = \sqrt{\gamma_{ij}dx^i dx^j} + N_i dx^i, \tag{58}$$

where $i, j = 1, 2, 3$ and γ_{ij} and N_i are defined accordingly as

$$\gamma_{ij}dx^i dx^j \equiv \frac{Y(r,\theta)}{X(r,\theta)}dr^2 + \frac{Z(r,\theta)}{X(r,\theta)}d\theta^2 + \frac{X(r,\theta)V(r,\theta) + U^2(r,\theta)}{A^2(r,\theta)}d\phi^2, \tag{59}$$

$$N_i dx^i \equiv -\frac{U(r,\theta)}{X(r,\theta)}d\phi. \tag{60}$$

The properties of the γ^{ij} are followed from the relation $\gamma^{ij}\gamma_{jk} = \delta^i{}_k$. γ_{ij} encodes the properties of a three-dimensional Riemannian space in which the trajectories of the null rays are described by the motion along a spatial curve.

Now, we use the metric (59) and then the Gauss-Bonnet theorem to have the definition of the light deflection angle, which is described as [68–70]

$$\alpha_D = -\int\int_{\substack{\infty \square \infty \\ O \quad S}} K dS + \int_S^O k_g dl, \tag{61}$$

where K is the curvature of the 3-surface along which light propagates, k_g is the geodesics curvature of the light curves, dS is the area element, and dl is the line element. We define the curvature of the 3-surface at the equatorial plane $(\theta = \pi/2)$ as

$$K = \frac{{}^3R_{r\phi r\phi}}{\gamma}, = \frac{1}{\sqrt{\gamma}}\left(\frac{\partial}{\partial\phi}\left(\frac{\sqrt{\gamma}}{\gamma_{rr}}{}^{(3)}\Gamma^{\phi}_{rr}\right) - \frac{\partial}{\partial r}\left(\frac{\sqrt{\gamma}}{\gamma_{rr}}{}^{(3)}\Gamma^{\phi}_{r\phi}\right)\right), \tag{62}$$

where γ is the determinant of the metric when $\theta = \pi/2$. For the rotating axially symmetric spacetime, Eq. (62) becomes [69,70]

$$K = -\sqrt{\frac{X^3}{Y(XV+U^2)}}\frac{\partial}{\partial r}\left[\sqrt{\frac{X^3}{Y(XV+U^2)}}\frac{\partial}{\partial r}\left(\frac{XV+U^2}{X^2}\right)\right]. \tag{63}$$

Therefore, K is evaluated to be

$$K = \left(\frac{3r_q^2}{2x^4} + \frac{3\epsilon r_q^2 + r_q^2 a^2}{x^6}\right) - \left(\frac{1}{x^3} + \frac{6a^2 + 3r_q^2 + 2\epsilon r_q^2}{x^5}\right)r_S + \left(\frac{3}{4x^4} + \frac{-6a^2 + \epsilon r_q^2 + 5r_q^2}{2x^6}\right)r_S^2 + \mathcal{O}\left(\frac{a^2\epsilon r_S^2}{x^8}, \frac{r_q^2\epsilon^2 r_S^2}{x^8}, \frac{a^2 r_q^2 r_S^2}{x^8}, \frac{r_S^3}{x^5}\right). \tag{64}$$

It is clear that to calculate the leading-order contribution we approximated the calculations to the weak-field limit, and all the higher-order terms are safely ignored. The Gaussian curvature is integrated over the quadrilateral which is closed so that [71]

$$\int\int_{\substack{\infty \square \infty \\ O \quad S}} K dS = \int_{\phi_S}^{\phi_O}\int_{\infty}^{x_0} K\sqrt{\gamma}\, dr d\phi, \tag{65}$$

where x_0 is the closest distance to the black hole. On utilizing Eqs. (17) and (18) and choosing $u = 1/x$, we can express the equation for light orbit as

$$\left(\frac{du}{d\phi}\right)^2 = F(u), \tag{66}$$

with

$$F(u) = \frac{u^4(XU+V^2)(U-2Vb-Xb^2)}{(Y(V+Xb))^2}, \tag{67}$$

with $b \equiv \ell/\mathcal{E}$ defined as the impact parameter. Using the weak-field solution $u = (\sin\phi)/b + \mathcal{O}(r_S, r_S^2)$ [71], Eq. (65) reduces to

$$\iint_{\infty\square\infty} KdS = \int_{\phi_S}^{\phi_O}\int_0^{\frac{\sin\phi}{b}} -\frac{K\sqrt{\gamma}}{u^2}\,dud\phi. \tag{68}$$

Therefore, for the metric (59), the integral (68) reads as

$$\begin{aligned}
\iint KdS =& \frac{r_S}{b}\left(\sqrt{1-b^2u_O^2}+\sqrt{1-b^2u_S^2}\right) + \frac{r_Sa^2}{3b^3}\left((2+b^2u_S^2)\sqrt{1-b^2u_S^2}+(2+b^2u_O^2)\sqrt{1-b^2u_O^2}\right)\\
&-\frac{r_Sr_q^2}{3b^3}\left((16+b^2u_S^2)\sqrt{1-b^2u_S^2}+(16+b^2u_O^2)\sqrt{1-b^2u_O^2}\right)\\
&-\frac{11a^2r_Sr_q^2}{25b^5}\left((3b^4u_S^4+4b^2u_S^2+8)\sqrt{1-b^2u_S^2}+(3b^4u_O^4+4b^2u_O^2+8)\sqrt{1-b^2u_O^2}\right)\\
&-\left(\frac{3r_q^2}{8b}+\frac{3r_S^2}{16b}\right)\left(u_S\sqrt{1-b^2u_S^2}+u_O\sqrt{1-b^2u_O^2}\right)\\
&-(\cos^{-1}bu_S+\cos^{-1}bu_O)\left(\frac{3r_q^2}{8b^2}+\frac{3a^2r_q^2}{8b^4}-\frac{15r_S^2}{16b^2}-\frac{9r_S^2a^2}{16b^4}-\frac{9\epsilon r_q^2}{16b^4}-\frac{27r_S^2r_q^2}{256b^4}\right)\\
&+\left(-\frac{a^2r_q^2}{8b^3}-\frac{15r_S^2a^2}{16b^3}-\frac{3\epsilon r_q^2}{8b^3}\right)\left(u_S(3+2b^2u_S^2)\sqrt{1-b^2u_S^2}+u_O(3+2b^2u_O^2)\sqrt{1-b^2u_O^2}\right)\\
&+\mathcal{O}\left(\frac{a^2r_q^2r_S^2}{b^6},\frac{r_q^2r_S^2\epsilon}{b^6},\frac{r_S^3}{b^3}\right),
\end{aligned} \tag{69}$$

where u_O and u_S are defined, respectively, as $\cos\phi_o = -\sqrt{1-b^2u_O^2}$, $\cos\phi_s = \sqrt{1-b^2u_S^2}$. The geodesic curvature of the manifold ${}^{(3)}\mathcal{M}$ is defined to be [71]

$$k_g = -\frac{1}{\sqrt{\gamma\gamma^{\theta\theta}}}N_{\phi,r}, \tag{70}$$

which reflects the fact the a nonrotating black hole does not contribute to it, thereby making a crucial contribution to the light deflection angle. Hence, the geodesic curvature for metric (59) reads

$$k_g = \left(\frac{a}{2x^4}-\frac{3a{r_q}^2}{4x^6}\right){r_S}^2+\left(\frac{a}{x^3}-\frac{3a{r_q}^2}{4x^5}\right)r_S-\frac{a{r_q}^2}{x^4}-\frac{4a\epsilon{r_q}^2}{x^6}+\mathcal{O}\left(\frac{r_S^3a}{x^5},\frac{ar_S^2r_q^2\epsilon}{x^8}\right). \tag{71}$$

We consider a coordinate system which is centered at the position of the lens, and we can take the approximation of the light curve such that $r = b/\cos\vartheta$ and $l = b\tan\vartheta$ [71]. Therefore, the geodesic curvature in its path integral form reads

$$\begin{aligned}
\int_S^O k_g dl =& \int_S^O\left(\left(\frac{a}{b^2}\cos\theta-\frac{3}{4}\frac{ar_q^2}{b^4}\cos^3\theta\right)r_S+\left(\frac{a}{2b^3}\cos^2\theta-\frac{3}{4}\frac{ar_q^2}{b^5}\cos^4\theta\right)r_S^2-\frac{ar_q^2}{b^3}\cos^2\theta-\frac{4a\epsilon r_q^2}{b^5}\cos^4\theta\right)d\theta+\mathcal{O}\left(\frac{r_S^3a}{b^4}\right)\\
=&-\frac{r_Sa}{b^2}\left(\sqrt{1-b^2u_S^2}+\sqrt{1-b^2u_O^2}\right)+\left(\frac{ar_q^2}{2b^2}-\frac{r_S^2a}{b^2}+\frac{9ar_qr_S^2}{32b^4}+\frac{3}{2}\frac{\epsilon ar_q^2}{b^4}\right)\left(u_S\sqrt{1-b^2u_S^2}+u_O\sqrt{1-b^2u_O^2}\right)\\
&+\left(\frac{ar_q^2}{2b^3}-\frac{r_S^2a}{4b^3}-\frac{45ar_q^2r_S^2}{32b^5}+\frac{3}{2}\frac{a\epsilon r_q^2}{b^5}\right)(\cos^{-1}bu_O+\cos^{-1}bu_S)\\
&-\frac{15ar_q^2r_S^2}{32b^4}\left(u_S(3+2b^2u_S^2)\sqrt{1-b^2u_S^2}+u_O(3+2b^2u_O^2)\sqrt{1-b^2u_O^2}\right)\\
&+\frac{\epsilon ar_q^2}{2b^4}\left(u_S(3+2b^2u_S^2)\sqrt{1-b^2u_S^2}+u_O(3+2b^2u_O^2)\sqrt{1-b^2u_O^2}\right)+\mathcal{O}\left(\frac{r_S^3a}{b^4},\frac{r_S^4ar_q^2}{b^7}\right),
\end{aligned} \tag{72}$$

In deriving the above expression, we adopted the prograde motion along the null geodesics ($dl > 0$), while for $dl < 0$, we obtain the retrograde motion with the extra terms with the "−" sign. For asymptotically large distances, we have $u_O \to 0$ and $u_S \to 0$, so the deflection angle gives us the expression

$$\alpha_D = \left(\frac{a\pi r_q^2}{2b^3} - \frac{3\pi r_q^2}{8b^2} - \frac{3\pi a^2 r_q^2}{8b^4} - \frac{9\epsilon\pi r_q^2}{16b^4} - \frac{3\epsilon a\pi r_q^2}{2b^5}\right) + \left(\frac{4}{b} - \frac{4a}{b^2} + \frac{8a^2}{3b^3} + \frac{32r_q^2}{6b^3} + \frac{176a^2 r_q^2}{50b^5}\right) r_S + \left(\frac{15\pi}{16b^2} - \frac{a\pi}{b^3} + \frac{9\pi a^2}{16b^4} + \frac{27\pi r_q^2}{256b^4} - \frac{45\pi a r_q^2}{32b^5}\right) r_S^2 + \mathcal{O}\left(\frac{r_S^3}{b^3}, \frac{r_S^4}{b^4}\right), \tag{73}$$

which reduces the Kerr-Newman limit of the deflection angle [50] when $\epsilon \to 0$, such that

$$\alpha_D^{\mathrm{KN}} = \left(\frac{a\pi r_q^2}{2b^3} - \frac{3\pi r_q^2}{8b^2} - \frac{3\pi a^2 r_q^2}{8b^4}\right) + \left(\frac{4}{b} - \frac{4a}{b^2} + \frac{8a^2}{3b^3} + \frac{32r_q^2}{6b^3} + \frac{176a^2 r_q^2}{50b^5}\right) r_S + \left(\frac{15\pi}{16b^2} - \frac{a\pi}{b^3} + \frac{9\pi a^2}{16b^4} + \frac{27\pi r_q^2}{256b^4} - \frac{45\pi a r_q^2}{32b^5}\right) r_S^2 + \mathcal{O}\left(\frac{r_S^3}{b^3}, \frac{r_S^4}{b^4}\right), \tag{74}$$

which in addition for $r_q \to 0$ reduces to the expression for the deflection angle for Kerr black holes [69,70]

$$\alpha_D^{\mathrm{Kerr}} = \left(\frac{4}{b} - \frac{4a}{b^2} + \frac{8a^2}{3b^3}\right) M + \left(\frac{15\pi}{4b^2} - \frac{a\pi}{b^3} + \frac{9\pi a^2}{4b^4}\right) M^2 + \mathcal{O}\left(\frac{M^3}{b^3}, \frac{M^4}{b^4}\right). \tag{75}$$

For the nonrotating ($a = 0$) black hole in EiBI theory, the deflection angle has the form

$$\alpha_D = \left(-\frac{3\pi r_q^2}{8b^2} - \frac{9\epsilon\pi r_q^2}{16b^4}\right) + \left(\frac{4}{b} + \frac{32r_q^2}{6b^3}\right) r_S + \left(\frac{15\pi}{16b^2} + \frac{27\pi r_q^2}{256b^4}\right) r_S^2 + \mathcal{O}\left(\frac{r_S^3}{b^3}, \frac{r_S^4}{b^4}\right). \tag{76}$$

VI. CONCLUSIONS

The general theory of relativity has been tested, and the theory incredibly matches with the local astrophysical evidences. The black holes are one of the strangest objects that were predicted in general relativity, but still there are only few concepts which have been verified on the experimental level. The experimental discovery that the black hole solutions such as Schwarzschild and Kerr metrics are not the actual real black holes would have pointed to a strong-field deviation from general relativity having deep implications at the fundamental level. In the present paper, we investigated the gravitational lensing in the strong-field approximation of the black holes in EiBI theory. Using the standard procedure for calculating the impact parameter, we study numerically the total azimuthal deflection α_D of light rays. We find that the charge parameter r_q and the Born-Infeld parameter ϵ influence the null geodesics. The coefficients p and q also have been obtained and plotted numerically, which shows that with fixed values of the charge r_q the coefficient p increases with rotation parameter a, while q is decreasing with a. Figure 3 shows that the coefficients p and q share the same property as those of Kerr-Newman ($\epsilon = 0$) and the stationary axially symmetric black holes in EiBI theory ($\epsilon \neq 0$). The deflection angle α_D showed monotonic behavior with the rotation parameter a, and it diverges at $u = u_m$, which has been shown with dots on the horizon lines in Fig. 4. As an application to the realistic scenario, we calculated the strong lensing observables s, θ_∞, and r_{mg} for SgrA* and M87 black holes.

We further calculate the weak-field gravitational lensing for the rotating black holes in EiBI theory. We have shown that in the limit $\epsilon \to 0$ our results match with the Kerr-Newman black holes. This way, all limit cases of Kerr black holes ($r_q = 0$) are satisfied. Our results may be important from a phenomenological point of view as the results from EHT slightly deviate from the Kerr black holes. This way, we can implement our investigations in the study of the astrophysical scenario.

ACKNOWLEDGMENTS

M. S. A.'s research is supported by the Institute Scheme for Innovative Research and Development (ISIRD) Grant No. 9-252/2016/IITRPR/708. The authors would like to thank Arpit Maurya for useful discussions and critical comments on the revised version of the manuscript.

[1] H. Stephani *et al.*, *Exact Solutions of Einstein's Field Equations*, Cambridge Monographs in Mathematical Physics, 2nd ed. (Cambridge University Press, Cambridge, England, 2003).
[2] B. Carter, Phys. Rev. Lett. **26**, 331 (1971).
[3] R. Penrose, Riv. Nuovo Cim. **1**, 252 (1969).
[4] R. Penrose, Gen. Relativ. Gravit. **34**, 1141 (2002).
[5] R. P. Kerr, Phys. Rev. Lett. **11**, 237 (1963).
[6] E. T. Newman, R. Couch, K. Chinnapared, A. Exton, A. Prakash, and R. Torrence, J. Math. Phys. (N.Y.) **6**, 918 (1965).
[7] S. Bhattacharya and A. Lahiri, Phys. Rev. D **83**, 124017 (2011).
[8] S. Bhattacharya, Gen. Relativ. Gravit. **48**, 128 (2016).
[9] J. Jiang, C. Bambi, and J. F. Steiner, J. Cosmol. Astropart. Phys. 05 (2015) 025.
[10] A. Cardenas-Avendano, J. Jiang, and C. Bambi, Phys. Lett. B **760**, 254 (2016).
[11] K. Akiyama *et al.*, Astrophys. J. **875**, L1 (2019).
[12] K. Akiyama *et al.*, Astrophys. J. **875**, L2 (2019).
[13] K. Akiyama *et al.*, Astrophys. J. **875**, L3 (2019).
[14] K. Akiyama *et al.*, Astrophys. J. **875**, L4 (2019).
[15] K. Akiyama *et al.*, Astrophys. J. **875**, L5 (2019).
[16] K. Akiyama *et al.*, Astrophys. J. **875**, L6 (2019).
[17] B. P. Abbott *et al.* (LIGO Scientific and Virgo Collaborations), Phys. Rev. Lett. **116**, 061102 (2016).
[18] B. P. Abbott *et al.* (LIGO Scientific and Virgo Collaborations), Phys. Rev. Lett. **119**, 141101 (2017).
[19] B. P. Abbott *et al.* (LIGO Scientific and Virgo Collaborations), Phys. Rev. Lett. **123**, 011102 (2019).
[20] C. Darwin, Proc. R. Soc. A **249**, 180 (1959).
[21] S. Frittelli, T. P. Kling, and E. T. Newman, Phys. Rev. D **61**, 064021 (2000).
[22] K. S. Virbhadra and G. F. R. Ellis, Phys. Rev. D **62**, 084003 (2000).
[23] V. Bozza, S. Capozziello, G. Iovane, and G. Scarpetta, Gen. Relativ. Gravit. **33**, 1535 (2001).
[24] V. Bozza, Phys. Rev. D **66**, 103001 (2002).
[25] C. Will, *Theory and Experiment in Gravitational Physics* (Cambridge University Press, Cambridge, England, 2018).
[26] A. Bhadra, Phys. Rev. D **67**, 103009 (2003).
[27] R. Whisker, Phys. Rev. D **71**, 064004 (2005).
[28] E. F. Eiroa, Phys. Rev. D **71**, 083010 (2005).
[29] Braz. J. Phys. **35**, 1113 (2005).
[30] C. R. Keeton and A. O. Petters, Phys. Rev. D **72**, 104006 (2005).
[31] C. R. Keeton and A. Petters, Phys. Rev. D **73**, 044024 (2006).
[32] S. V. Iyer and A. O. Petters, Gen. Relativ. Gravit. **39**, 1563 (2007).
[33] P. Zhang, M. Liguori, R. Bean, and S. Dodelson, Phys. Rev. Lett. **99**, 141302 (2007).
[34] S. b. Chen and J. l. Jing, Phys. Rev. D **80**, 024036 (2009).
[35] R. Reyes, R. Mandelbaum, U. Seljak, T. Baldauf, J. E. Gunn, L. Lombriser, and R. E. Smith, Nature (London) **464**, 256 (2010).
[36] S. W. Wei, Y. X. Liu, C. E. Fu, and K. Yang, J. Cosmol. Astropart. Phys. 10 (2012) 053.
[37] V. Bozza and G. Scarpetta, Phys. Rev. D **76**, 083008 (2007).
[38] E. F. Eiroa and C. M. Sendra, Classical Quantum Gravity **28**, 085008 (2011).
[39] J. Sadeghi and H. Vaez, J. Cosmol. Astropart. Phys. 06 (2014) 028.
[40] K. Sarkar and A. Bhadra, Classical Quantum Gravity **23**, 6101 (2006).
[41] M. S. Ali and S. Bhattacharya, Phys. Rev. D **97**, 024029 (2018).
[42] S. Bhattacharya and S. Chakraborty, Phys. Rev. D **95**, 044037 (2017).
[43] K. S. Virbhadra and C. R. Keeton, Phys. Rev. D **77**, 124014 (2008).
[44] J. Man and H. Cheng, J. Cosmol. Astropart. Phys. 11 (2014) 025.
[45] W. Javed, R. Babar, and A. Ovgun, Phys. Rev. D **99**, 084012 (2019).
[46] R. Shaikh, P. Banerjee, S. Paul, and T. Sarkar, Phys. Rev. D **99**, 104040 (2019).
[47] I. Z. Stefanov, S. S. Yazadjiev, and G. G. Gyulchev, Phys. Rev. Lett. **104**, 251103 (2010).
[48] V. Cardoso, A. S. Miranda, E. Berti, H. Witek, and V. T. Zanchin, Phys. Rev. D **79**, 064016 (2009).
[49] S. Hod, Phys. Rev. D **80**, 064004 (2009).
[50] R. Kumar, S. G. Ghosh, and A. Wang, Phys. Rev. D **100**, 124024 (2019).
[51] R. Kumar, B. P. Singh, and S. G. Ghosh, Ann. Phys. (Amsterdam) **420**, 168252 (2020).
[52] R. Kumar, S. G. Ghosh, and A. Wang, Phys. Rev. D **101**, 104001 (2020).
[53] S. U. Islam, R. Kumar, and S. G. Ghosh, J. Cosmol. Astropart. Phys. 09 (2020) 030.
[54] C. H. Ohanian, Am. J. Phys. **55**, 428 (1987).
[55] A. Einstein, Science **84**, 506 (1936).
[56] K. S. Virbhadra and G. F. R. Ellis, Phys. Rev. D **65**, 103004 (2002).
[57] R. Gavazzi, T. Treu, L. V. E. Koopmans, A. S. Bolton, L. A. Moustakas, S. Burles, and P. J. Marshall, Astrophys. J. **677**, 1046 (2008).
[58] V. Bozza, Phys. Rev. D **67**, 103006 (2003).
[59] R. Kumar, S. U. Islam, and S. G. Ghosh, Eur. Phys. J. C **80**, 1128 (2020).
[60] C. Bambi, K. Freese, S. Vagnozzi, and L. Visinelli, Phys. Rev. D **100**, 044057 (2019).
[61] D. Psaltis *et al.*, Phys. Rev. Lett. **125**, 141104 (2020).
[62] S. U. Islam and S. G. Ghosh, Phys. Rev. D **103**, 124052 (2021).
[63] S. G. Ghosh, R. Kumar, and S. U. Islam, J. Cosmol. Astropart. Phys. 03 (2021) 056.
[64] M. Guerrero, G. Mora-Pérez, G. J. Olmo, E. Orazi, and D. Rubiera-Garcia, J. Cosmol. Astropart. Phys. 07 (2020) 058.
[65] S. Chandrasekhar, *The Mathematical Theory of Black Holes* (Oxford University Press, New York, 1992).
[66] J. Kormendy and L. C. Ho, Annu. Rev. Astron. Astrophys. **51**, 511 (2013).
[67] T. Do *et al.*, Science **365**, 664 (2019).
[68] G. W. Gibbons and M. C. Werner, Classical Quantum Gravity **25**, 235009 (2008).
[69] A. Ishihara, Y. Suzuki, T. Ono, T. Kitamura, and H. Asada, Phys. Rev. D **94**, 084015 (2016).
[70] A. Ishihara, Y. Suzuki, T. Ono, and H. Asada, Phys. Rev. D **95**, 044017 (2017).
[71] T. Ono, A. Ishihara, and H. Asada, Phys. Rev. D **96**, 104037 (2017).